Is it possible to use the green coronal line instead of X rays to cancel an effect of the coronal emissivity deficit in estimation of the prominence total mass from decrease of the EUV-corona intensities?

P. Schwartz,[1] P. Heinzel,[2] S. Jejčič,[3] J. Rybák,[1] P. Kotrč,[2] F. Fárník,[2] Yu.A. Kupryakov,[4,2] E.E. Deluca,[5] L. Golub,[5] P.R. Jibben,[5] U. Anzer,[6] A.G. Tlatov,[7] and S.A. Guseva[7]

[1]*Astronomical Institute of Slovak Academy of Sciences, 05960 Tatranská Lomnica, Slovak Republic;* pschwartz@astro.sk

[2]*Astronomical Institute, Academy of Sciences of the Czech Republic, 25165 Ondřejov,Czech Republic*

[3]*University of Ljubljana, Faculty of Mathematics and Physics, 1000 Ljubljana, Slovenija*

[4]*Sternberg Astronomical Institute, Moscow University, 119899 Moscow, Russia*

[5]*Harvard-Smithonian Center for Astrophysics, 60 Garden Street, MA 02138 Cambridge, USA*

[6]*Max-Planck-Institut für Astrophysik, Karl-Schwarzschild-Strasse 1, 85740 Garching, Germany*

[7]*Kislovodsk Mountain Astronomical Station of the Pulkovo observatory, Gagarina 100, 357700 Kislovodsk, Russia*

Abstract. Total masses of six quiescent prominences observed from April through June 2011 were estimated using multi-spectral observations (in EUV, X-rays, Hα, and Ca II H). The method for the total mass estimation is based on the fact that the intensity of the EUV solar corona at wavelengths below 912 Å is reduced at a prominence by the absorption in resonance continua (photoionisation) of hydrogen and possibly by helium and subsequently an amount of absorbed radiation is proportional to the column density of hydrogen and helium plasma. Moreover, the deficit of the coronal emissivity in volume occupied by the cool prominence plasma also contributes to the intensity decrease. The observations in X-rays which are not absorbed by the prominence plasma, allow us to separate these two mechanisms from each other. The X-ray observations of XRT onboard the Hinode satellite made with the Al-mesh focal filter were used because the X-ray coronal radiation formed in plasma of temperatures of the order of 10^6 K was registered and EUV spectral lines occurring in the 193, 211 and 335 Å channels of the Atmospheric Imaging Assembly of the Solar Dynamics Observatory satellite are also formed at such temperatures. Unfortunately, the Al-mesh filter has a secondary peak of the transmittance at around 171 Å which causes a contribution from the EUV corona to the measured data of up to 11 % in the quiet corona. Thus, absorption in prominence plasma influences XRT X-ray data when using the Al-mesh filter. On the other hand, other X-ray XRT filters are more sensitive to plasma of much higher temperatures ($\log T$ of the order of 7), thus observations using these filters cannot be used together with the AIA observations in the method for mass estimations. This problem could be

solved using observations in the green coronal line instead of X-rays. Absorption of the green coronal line by a prominence plasma is negligible and this line is formed at temperatures of the order of 10^6 K. We compare values of the total mass of the prominence observed on 20 October 2012 on the SE limb estimated when using XRT X-ray observations and observations in the green coronal line obtained at Kislovodsk Mountain Astronomical Station of the Pulkovo observatory (Russia).

1. Introduction

In the last two decades multi-spectral observations in UV, EUV, and X-ray from space together with ground-based optical observations made it possible to estimate reliably the total mass of prominences. One possibility would be to estimate the column mass of hydrogen and/or helium plasma in prominences using spectral observations of UV and visible lines of hydrogen and helium (Balmer and Lyman lines) and sophisticated models in which plasma is assumed not to be in the state of *local thermodynamic equilibrium* (hereafter referred to as NLTE models; see e.g. Labrosse et al. 2010 and references therein). The problem can be a rather high complexity of such NLTE models which depend on various free parameters. Another possibility is to infer the column mass and subsequently the total mass from the amount of radiation absorbed by the photoionisation in the prominence plasma at resonance continua of hydrogen and helium. This estimation of the mean column mass of prominences observed near the limb was first made by Kucera et al. (1998) using EUV observations from the *Coronal Diagnostic Spectrometer* (CDS) (Harrison et al. 1995) on board the *Solar and Heliospheric Observatory* (SoHO) satellite. The advantage of the observations used by Kucera et al. (1998) was that CDS as a spectrograph observed only in spectral lines of interest, but spectrographs are able to obtain spectra from only one slit position during one exposure. Larger fields of view can be scanned by the spectrograph slit, as the CDS does, for example, but in such a case, intensities in different slit positions the scan is composed of were obtained at different times. The first estimation of the prominence mass using filtergrams was made by Golub et al. (1999) using *Transition Region and Coronal Explorer* (TRACE, `http://trace.lmsal.com`) data. Later, similar studies were made by Gilbert et al. (2005, 2006) using observations of the *EUV Imaging Telescope* (EIT) (Delaboudinière et al. 1995) on board SoHO in the 195 Å channel and more recently by Williams et al. (2013) who used observations from the *Atmospheric Imaging Assembly* (AIA) instrument (Lemen et al. 2012) on board the *Solar Dynamics Observatory* (SDO) in several EUV coronal channels of wavelengths below 228 Å (head of the resonance continuum of He II). In our estimations of the total mass of a prominence we also use AIA observations and hydrogen column densities and subsequently the total mass of a prominence is obtained from the amount of EUV coronal radiation absorbed by the prominence plasma in resonance continua of hydrogen and helium. But except of the absorption, a coronal emissivity deficit is assumed because it can contribute remarkably to the coronal intensity depression at a prominence position (Anzer & Heinzel 2005). The coronal emissivity deficit is caused by the presence of cool and/or low-density material in volume occupied by the prominence or its cavity, which causes a lowering or even a lack of coronal emissivity in such a volume. To eliminate an effect of the coronal emissivity deficit, observations in spectral lines or spectral region not absorbed by the prominence plasma are used, e.g. in X-rays as proposed by Anzer et al. (2007).

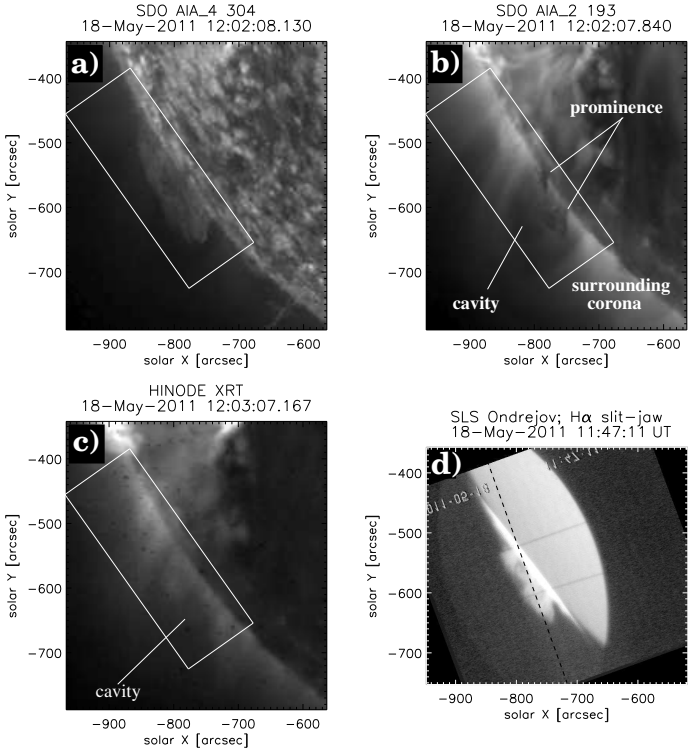

Figure 1. Observations of the prominence of 18 May 2011: Cut-offs from the full-disc observations from the AIA instrument in the 304 Å, 193 Å channels, and of the XRT telescope obtained using the Al-mesh filter are shown in the panels a – c. Rectangles drawn by a solid white line mark areas of interest. The SLS spectrograph Hα slit-jaw image co-aligned with AIA observations is shown in panel d. One of the eight slit positions is plotted by a black inclined dashed line.

2. Estimation of the total mass using EUV and X-ray observations

More than 30 quiescent prominences were observed during a campaign held from April through June 2011. Prominences were selected according to Hα observations of two ground-based multi-camera spectrographs at the Ondřejov observatory: SLS (*Solar Laboratory Spectrograph*) (see SLS web page `http://radegast.asu.cas.cz/MFS/prominence_archiv/sls.html`) and HSFA2 (*Horizontal Sonnen Forschung Anlage No. 2*) (Kotrč 2009). The HSFA2 instrument was observing also in the Ca II H line (λ 3968 Å) and three other lines. Observations from these two instruments are hereafter referred to as GBO. X-ray full-disc images obtained by the XRT (*X-ray telescope*) instrument (Golub et al. 2007) on board the *Hinode* satellite (Kosugi et al. 2007) on the same day as the SLS observations were used as well. As the AIA instrument on board the SDO satellite records images in all channels with very high cadence (approximately every 12 s), it is almost always possible to find quasi-simultaneous EUV full-disc observations. Thus it was not necessary to include the AIA instrument into the observing campaign. Till now, the total mass of only six prominences obtained between 19 April and 18 May during the campaign were estimated. As an example, the prominence observations from 18 May 2011 are shown in Fig. 2.

The method of Heinzel et al. (2008) was used to estimate the optical thickness of hydrogen and helium prominence plasma from the decrease of EUV intensity at a prominence. When a tangential to the solar limb cut through a prominence in the AIA 193 Å and X-ray XRT image is made, a dip at the prominence position in the intensity distributions along the cut occurs both in EUV and X-ray data. The intensity decrease at a prominence is deeper in EUV than in X-rays because both absorption and emissivity deficit affect EUV radiation while X-ray radiation is reduced only by the emissivity deficit. But in the cavity and surrounding quiet corona both the EUV and the X-ray intensity distributions are similar. And thus, it is necessary to multiply the X-ray intensity distribution by a specific factor to fit EUV data in the cavity and corona. And then optical thickness τ_{EUV} in EUV is proportional to the ratio r' of EUV and fitted X-ray

$$\tau_{\mathrm{EUV}} = -\ln\left(1 - \frac{1 - r'}{\alpha}\right), \tag{1}$$

where α is a factor of asymmetry of coronal emissivity along the line of sight in front and behind the prominence. Using a theoretical formula for τ_{EUV} calculation published, e.g., by Anzer & Heinzel (2005), values of hydrogen column density can be derived from τ_{EUV} when ionisation degrees of hydrogen and neutral and singly ionised helium are known. The ionisation degree of hydrogen is determined from the Hα and Ca II H line profiles using a simple cloud model (Beckers 1964) and 1D isobaric and isothermal models of Heinzel et al. (1994). Ionisation degrees of helium are estimated iteratively comparing ratios of optical thickness estimated from AIA data in the 193 Å, 211 Å, and 335 Å channels with values calculated theoretically. Finally, the total mass of a prominence is obtained by integration of hydrogen column mass throughout the whole prominence and then multiplied by 1.4 (adopting a common solar helium abundance of 0.1 and assuming that the mass of the helium atom is 4 times the mass of a hydrogen atom). XRT observations made with the Al-mesh were used because this filter transmits mainly radiation emitted from plasma at a temperature of $\sim 10^6$ K which emits also EUV radiation registered by AIA data in the 193 Å, 211 Å, and 335 Å channels. For other XRT filters it registers radiation emitted from plasma of temperatures of the order of magnitude 10^7. It is also important to note that the Al-mesh filter has a secondary peak at 171 Å. Thus, the X-ray signal is contaminated by EUV radiation but this contamination does not exceed 25 %. This problem is examined in more detail in the next section. The total mass estimated for the six chosen prominences corrected for the EUV contamination of XRT Al-mesh X-ray data ranges from 3.7×10^{11} up to 1.8×10^{12} kg. More details about observation of the six prominences and the method can be found in the work of Schwartz et al. (2015a).

3. Problems of using XRT X-ray observations in the mass estimation

In our method for the estimation of the total mass of prominences it was assumed that X-rays are not absorbed by the hydrogen and helium prominence as it was already investigated by Anzer et al. (2007). But they examined the absorption at 50 Å where the Soft X-ray (SXR) telescope of the Yohkoh satellite has a maximum of sensitivity. But all filters of the XRT telescope have a maximum of transmittance at 10 Å (Golub et al. 2007) where except of hydrogen and helium also continua of other elements such as C, N, O, Ne, Mg, Si, S and Fe occur. The hypothesis of the absorption at 10 Å is supported by the fact that the spine of the prominence observed at the NW limb on 22 June 2010 is

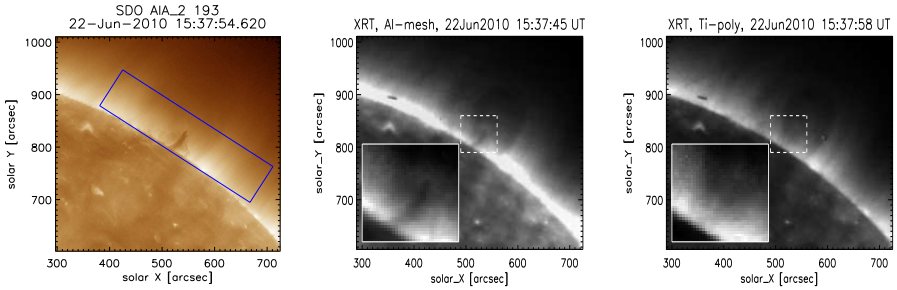

Figure 2. Observations of the prominence made on 22 Jun 2010 by AIA in the 193 Å channel (*left*) and in X rays by XRT using the Al-mesh (*middle*) and Ti-poly filters (*right*).

seen as a dark structure not only in the AIA 193 Å image but also in the Al-mesh XRT image shown on the left and middle panels of Fig.2, respectively. It is visible faintly also in the Ti-poly filter image shown in the right panel of the figure. In our work Schwartz et al. (2015b) we calculated the continuum optical thickness of a prominence plasma composed of hydrogen, helium and heavier elements for wavelengths within 1 – 50 Å and three values of the hydrogen column density – 10^{17}, 10^{19} and 10^{21} cm^{-2}. Values of the optical thickness are increasing with the column density. We found that even at such high hydrogen column density as 10^{21} cm^{-2}, the optical thickness at 5 Å is only 0.01. Using the method described in the previous section, Gunár et al. (2014) calculated hydrogen column density for the prominence of 22 June 2010 and the maximum value of 10^{19} cm^{-2} was found for which the optical thickness is even smaller. For neither of the six prominences from 2011, the hydrogen column density exceeds this limit. Another reason for the dark manifestation of the prominence spine in the XRT images could be a secondary peak of the filter transmittance at 171 Å. For the Al-mesh filter a contribution to the measured XRT signal from the EUV radiation in the quiet corona is around 11 % while it is only 7 –9 % at the spine due to absorption of EUV radiation by the prominence plasma. It means that 16 –20 % of the darkening at the spine originates from the EUV contamination (Schwartz et al. 2015b). But what is the nature of the remaining 80 %? Moreover, for the Ti-poly filter the EUV contamination is below the noise. Thus, the only explanation is the effect of a considerable coronal emissivity deficit caused by a very large geometrical size of the spine along the line of sight. The size of 10^5 km estimated from the XRT observations by Schwartz et al. (2015b) agrees with observations of the STEREO-A satellite, where the spine of the prominence is seen as a filament.

4. The green coronal line instead of X-rays in the mass estimation

Thus, there is a non-negligible EUV contamination of the XRT X-ray data obtained with the Al-mesh filter and on the other hand a plasma of one order of magnitude higher temperature is observed with other XRT filters and therefore not suitable for the mass estimations. Moreover, XRT filters have been degrading very fast in the last three years and gradually more contamination spots are appearing in the XRT data. Because the absorption of the green coronal line by the prominence plasma is also negligible it can be used instead of X-rays in our method for the mass estimation. Observations of a

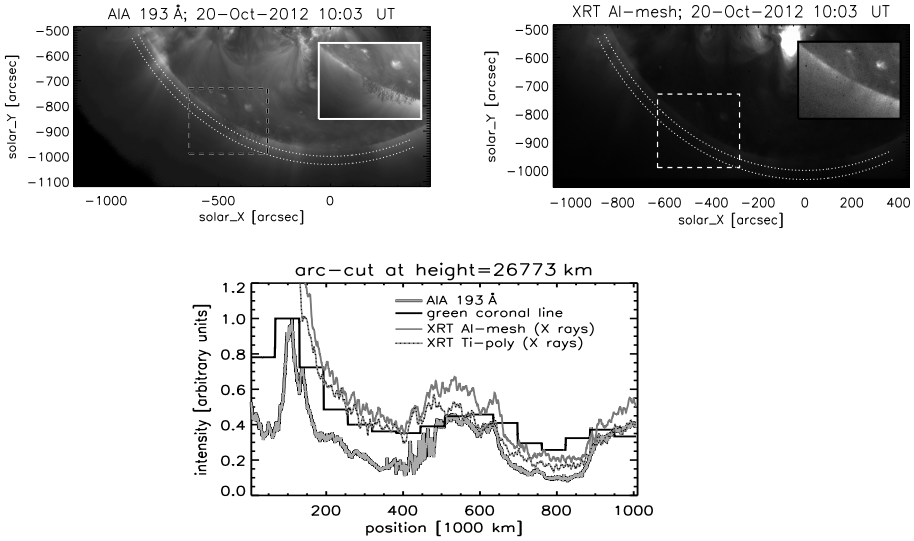

Figure 3. Observations of a prominence and its cavity on the SE limb on 20 October 2012 by AIA in the 193 Å channel (*top left*), XRT in X-rays (*top right*), and comparison of distributions along an arched cut of EUV, X-ray and green-coronal--line intensities (*bottom*).

prominence on SE limb made by AIA in the 193 Å channel and by XRT in X-rays using the Al-mesh filter are shown in Fig. 3. As intensities of the green coronal line observed at the Kislovodsk Mountain Astronomical Station of the Pulkovo observatory in Russia were obtained only for heights above the solar surface around 27 000 km (Makarov et al. 2006), just an arched cut at the height of 26 773 km was made and intensities along the cut were plotted in the right panel of Fig. 3. Notice the similar behaviour of the Ti--poly and green-coronal line intensities at the prominence and quiet Sun (QS) while the Al-mesh data are somewhat lower at positions 300 000 – 400 000 km most probable because of the EUV contamination.

5. Conclusion

Comparison of distributions of intensities of X-rays and the green coronal line along the cut shown in the right panel of Fig. 3 suggests that the green coronal line data could be used instead of X-rays. But still more investigations in this field must be done and mainly observations of the green coronal line in a larger FOV are necessary. We will be able to obtain such data in the near future from the Lomnický Peak Observatory in Slovakia.

Acknowledgments. This work was supported by the Slovak Research and Development Agency under the contract No. APVV-0816-11 and by the Science Grant Agency project VEGA 2/0004/16. The AIA data are courtesy of NASA/SDO and the AIA science team.

References

Anzer, U., & Heinzel, P. 2005, ApJ, 622, 714

Anzer, U., Heinzel, P., & Fárnik, F. 2007, Solar Phys., 242, 43
Beckers, J. M. 1964, Ph.D. thesis, Sacramento Peak Observatory, Air Force Cambridge Research Laboratories, Mass., USA
Delaboudinière, J.-P., Artzner, G. E., Brunaud, J., Gabriel, A. H., Hochedez, J. F., Millier, F., Song, X. Y., Au, B., Dere, K. P., Howard, R. A., Kreplin, R., Michels, D. J., Moses, J. D., Defise, J. M., Jamar, C., Rochus, P., Chauvineau, J. P., Marioge, J. P., Catura, R. C., Lemen, J. R., Shing, L., Stern, R. A., Gurman, J. B., Neupert, W. M., Maucherat, A., Clette, F., Cugnon, P., & van Dessel, E. L. 1995, Solar Phys., 162, 291
Gilbert, H. R., Falco, L. E., Holzer, T. E., & MacQueen, R. M. 2006, ApJ, 641, 606
Gilbert, H. R., Holzer, T. E., & MacQueen, R. M. 2005, ApJ, 618, 524
Golub, L., Bookbinder, J., Deluca, E., Karovska, M., Warren, H., Schrijver, C. J., Shine, R., Tarbell, T., Title, A., Wolfson, J., Handy, B., & Kankelborg, C. 1999, Physics of Plasmas, 6, 2205
Golub, L., Deluca, E., Austin, G., Bookbinder, J., Caldwell, D., Cheimets, P., Cirtain, J., Cosmo, M., Reid, P., Sette, A., Weber, M., Sakao, T., Kano, R., Shibasaki, K., Hara, H., Tsuneta, S., Kumagai, K., Tamura, T., Shimojo, M., McCracken, J., Carpenter, J., Haight, H., Siler, R., Wright, E., Tucker, J., Rutledge, H., Barbera, M., Peres, G., & Varisco, S. 2007, Solar Phys., 243, 63
Gunár, S., Schwartz, P., Dudík, J., Schmieder, B., Heinzel, P., & Jurčák, J. 2014, A&A, 567, A123
Harrison, R. A., Sawyer, E. C., Carter, M. K., Cruise, A. M., Cutler, R. M., Fludra, A., Hayes, R. W., Kent, B. J., Lang, J., Parker, D. J., Payne, J., Pike, C. D., Peskett, S. C., Richards, A. G., Gulhane, J. L., Norman, K., Breeveld, A. A., Breeveld, E. R., Al Janabi, K. F., McCalden, A. J., Parkinson, J. H., Self, D. G., Thomas, P. D., Poland, A. I., Thomas, R. J., Thompson, W. T., Kjeldseth-Moe, O., Brekke, P., Karud, J., Maltby, P., Aschenbach, B., Bräuninger, H., Kühne, M., Hollandt, J., Siegmund, O. H. W., Huber, M. C. E., Gabriel, A. H., Mason, H. E., & Bromage, B. J. I. 1995, Solar Phys., 162, 233
Heinzel, P., Gouttebroze, P., & Vial, J.-C. 1994, A&A, 292, 656
Heinzel, P., Schmieder, B., Fárník, F., Schwartz, P., Labrosse, N., Kotrč, P., Anzer, U., Molodij, G., Berlicki, A., DeLuca, E. E., Golub, L., Watanabe, T., & Berger, T. 2008, ApJ, 686, 1383
Kosugi, T., Matsuzaki, K., Sakao, T., Shimizu, T., Sone, Y., Tachikawa, S., Hashimoto, T., Minesugi, K., Ohnishi, A., Yamada, T., Tsuneta, S., Hara, H., Ichimoto, K., Suematsu, Y., Shimojo, M., Watanabe, T., Shimada, S., Davis, J. M., Hill, L. D., Owens, J. K., Title, A. M., Culhane, J. L., Harra, L. K., Doschek, G. A., & Golub, L. 2007, Solar Phys., 243, 3
Kotrč, P. 2009, Central European Astrophysical Bulletin, 33, 327
Kucera, T. A., Andretta, V., & Poland, A. I. 1998, Solar Phys., 183, 107
Labrosse, N., Heinzel, P., Vial, J.-C., Kucera, T., Parenti, S., Gunár, S., Schmieder, B., & Kilper, G. 2010, Space Sci.Rev., 151, 243
Lemen, J. R., Title, A. M., Akin, D. J., Boerner, P. F., Chou, C., Drake, J. F., Duncan, D. W., Edwards, C. G., Friedlaender, F. M., Heyman, G. F., Hurlburt, N. E., Katz, N. L., Kushner, G. D., Levay, M., Lindgren, R. W., Mathur, D. P., McFeaters, E. L., Mitchell, S., Rehse, R. A., Schrijver, C. J., Springer, L. A., Stern, R. A., Tarbell, T. D., Wuelser, J.-P., Wolfson, C. J., Yanari, C., Bookbinder, J. A., Cheimets, P. N., Caldwell, D., Deluca, E. E., Gates, R., Golub, L., Park, S., Podgorski, W. A., Bush, R. I., Scherrer, P. H., Gummin, M. A., Smith, P., Auker, G., Jerram, P., Pool, P., Soufli, R., Windt, D. L., Beardsley, S., Clapp, M., Lang, J., & Waltham, N. 2012, Solar Phys., 275, 17
Makarov, V. I., Tlatov, A. G., & Callebaut, D. K. 2006, Solar Phys., 237, 201
Schwartz, P., Heinzel, P., Kotrč, P., Fárník, F., Kupryakov, Y. A., DeLuca, E. E., & Golub, L. 2015a, A&A, 574, A62
Schwartz, P., Jejčič, S., Heinzel, P., Anzer, U., & Jibben, P. R. 2015b, ApJ, 807, 97
Williams, D. R., Baker, D., & van Driel-Gesztelyi, L. 2013, ApJ, 764, 165